

# Boundary chromatic polynomial

Jesper Lykke Jacobsen<sup>1,2</sup> and Hubert Saleur<sup>2,3</sup>

<sup>1</sup>Université Pierre et Marie Curie, 4 place Jussieu,  
75252 Paris Cedex 05, France

<sup>2</sup> Institut de Physique Théorique, CEA Saclay,  
91191 Gif-sur-Yvette, France

<sup>3</sup> Department of Physics and Astronomy,  
University of Southern California,  
Los Angeles, CA 90089, USA

November 26, 2018

## Abstract

We consider proper colorings of planar graphs embedded in the annulus, such that vertices on one rim can take  $Q_s$  colors, while all remaining vertices can take  $Q$  colors. The corresponding chromatic polynomial is related to the partition function of a boundary loop model. Using results for the latter, the phase diagram of the coloring problem (with real  $Q$  and  $Q_s$ ) is inferred, in the limits of two-dimensional or quasi one-dimensional infinite graphs. We find in particular that the special role played by Beraha numbers  $Q = 4 \cos^2 \frac{\pi}{n}$  for the usual chromatic polynomial does not extend to the case  $Q \neq Q_s$ . The agreement with (scarce) existing numerical results is perfect; further numerical checks are presented here.

## 1 Introduction

Let  $G = (V, E)$  be a planar graph embedded in the annulus. Let  $V_s \subseteq V$  be the subset of vertices surrounding the face that contains the point at infinity. In other words,  $V_s$  are the vertices on the outer rim of the annulus.

Place a spin variable  $\sigma_i = 1, 2, \dots, Q$  on each bulk vertex ( $i \in V \setminus V_s$ ) and a boundary spin  $\sigma_j = 1, 2, \dots, Q_s$  on each boundary vertex ( $j \in V_s$ ). We suppose initially that  $Q_s \leq Q$ , so that  $Q - Q_s$  of the colors allowed for the bulk spins are forbidden for the boundary spins.

The Potts model partition function  $Z_G(Q, Q_s; \mathbf{v})$ —also known to graph theorists as the multivariate Tutte polynomial—can be defined through a slight generalization of the usual Fortuin-Kasteleyn expansion [1]

$$Z_G(Q, Q_s; \mathbf{v}) = \sum_{A \subseteq E} Q^{k(A)} \left( \frac{Q_s}{Q} \right)^{k_s(A)} \prod_{e \in A} v_e \quad (1)$$

where  $k(A)$  is the number of all connected components (clusters) in the graph induced by the edge subset  $A$ , and  $k_s(A)$  is the number of connected components that contain at least one vertex from  $V_s$ . In other words,  $Q_s$  (resp.  $Q$ ) is the weight of a cluster that contains at least one (resp. does not contain any) vertex in  $V_s$ . The edge variables  $\mathbf{v} = \{v_e\}_{e \in E}$  are related to the usual spin-spin couplings  $K_e$  through the relation  $v_e = \exp(K_e) - 1$ .

Note that in (1) there is no need for  $Q$  and  $Q_s$  to be integers, nor do we have to impose the constraint  $Q_s \leq Q$ . We shall henceforth promote (1) to the *definition* of the (boundary) Potts model [2].

In this paper we wish to study the problem of proper colorings of  $G$ , such that bulk vertices can have  $Q$  different colors, whereas boundary vertices can have only a subset of  $Q_s$  colors. Adjacent vertices (of whatever type) are constrained to have different colors. The partition function  $Z_G(Q, Q_s; -1)$ , i.e. with all  $v_e = -1$ , counting the number of such proper colorings is referred to as the *boundary chromatic polynomial* and denoted  $P_G(Q, Q_s)$ . Note that  $P_G(Q, Q)$  is nothing else than the usual chromatic polynomial, which has been studied extensively in the literature [3].

We address in particular the issue of the phase diagram of  $P_G(Q, Q_s)$  for “large graphs”—what is meant precisely by this will be discussed below. The main result is the location and nature of a series of phase transition (with corresponding behaviors of zeroes of  $P_G$ ) occurring when one varies one or both of the parameters  $Q$  and  $Q_s$ . We emphasize that most of our results are quite general, and do not depend on the detailed structure of the underlying graph  $G$ .

In the usual case  $Q = Q_s$ , one of the striking features of the chromatic polynomial is that for “large graphs” its real zeroes possess accumulation

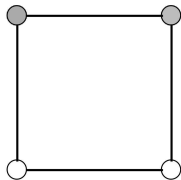


Figure 1: For this graph (with the shaded vertices on the boundary) the chromatic polynomial continued from the region  $Q \geq Q_s$  is  $P_G = (Q^2 - 3Q + 3)Q_s(Q_s - 1)$ . It does not vanish for  $Q = 0$  nor  $Q = 1$ . Meanwhile the chromatic polynomial continued from the region  $Q \leq Q_s$  is obtained—in this simple example—by exchanging  $Q$  and  $Q_s$  in the above expression, and does vanish for  $Q = 0$  and  $Q = 1$ .

points which belong to the magic set of Beraha numbers:

$$B_t = 4 \cos^2 \left( \frac{\pi}{t} \right) \quad \text{for } t = 2, 3, \dots \quad (2)$$

Note that the first two such numbers are  $Q = 0$  and  $Q = 1$ , which are usually exact zeroes for finite graphs as well. One of the striking conclusions of our study is that the special role played by Beraha numbers is not very resistant to changing  $Q_s$ . Depending on the problem one chooses, there can indeed be accumulating zeroes at other special points of the real axis.

It is important to realize that the definition of  $P_G(Q, Q_s)$ , albeit very natural, can lead to counterintuitive features in particular when interpreted outside the initial domain of definition  $Q_s \leq Q$ . For instance it turns out that for most graphs,  $P_G(Q, Q_s)$  does not vanish when  $Q = 0$  or  $Q = 1$ , even though in that case there is no way—forgetting the boundary contribution—to color the bulk vertices with  $Q$  colors. The point is that in the original definition (1), spins belonging to clusters that touch the boundary receive a fugacity  $Q_s$ , which initially is assumed smaller or equal to  $Q$ , but which, after continuation, can in fact be greater, hence “pumping” the number of colors in the bulk. Fig. 1 provides a simple example of this subtlety.

One could define another chromatic polynomial starting from the situation where  $Q \leq Q_s$ . In terms of the subsequent cluster and loop model expansions, it would however be much less interesting. Indeed, in such a model, only clusters not containing any of the bulk spins would get the fu-

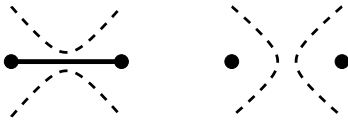


Figure 2: The transition system (shown as dashed lines) depends on whether a given edge  $e$  (shown as a solid line) is present in [left panel] or absent from [right panel] the edge subset  $A \subseteq E$  in (3).

gacity  $Q_s$ , and thus only loops “glued to the boundary” would get a fugacity different from the bulk ones. This presumably would not affect the patterns of zeroes.

The layout of the paper is as follows. In section 2 we relate the boundary chromatic polynomial to a loop model which was previously introduced in [2] and further studied in [4]. In section 3 the issue of the phase diagram is transposed into the setting of the Beraha-Kahane Weiss theorem [6] which we review. The necessary input for applying that theorem is supplied by an analytic continuation of the field theoretic results of [2], as explained in section 4. Here we also arrive at the main results of the paper, which are the phase transition loci (15)–(16). All of this applies to the two-dimensional thermodynamic limit. However, the main results remain valid for quasi one-dimensional graphs, and we provide the necessary arguments in section 5. A few numerical validations of our results are given in section 6 after which we present our conclusions.

## 2 Boundary loop model

The cluster model (1) can obviously be defined for any graph  $G$ . However, when  $G$  is planar, the cluster model can be turned into a loop model on the medial graph  $\mathcal{M}$ .

We recall that the medial (or surrounding) graph has a vertex standing on each edge  $e \in E$ , and an edge between vertices standing on edges  $e_1, e_2$ , whenever  $e_1, e_2$  are incident to a common vertex in  $V$  and surround a common face in  $G$ .

A non-intersecting transition system on  $\mathcal{M}$  is defined locally as in Fig. 2. Globally, this transition system is a set of loops—or cycles in the standard graph theoretical terminology—which separate clusters in  $G$  from their duals. By the existence of a point at infinity, the inside and outside of a loop are

well defined. A loop that contains at least one vertex of  $V_s$  on its inside is called a boundary loop. A loop that is not a boundary loop is called a bulk loop.

Let now  $\ell(A)$  be the total number of loops, and  $\ell_s(A)$  the number of boundary loops. By the Euler relation, one has  $k(A) = \frac{1}{2}(\ell(A) + |V| - |E|)$ , so that

$$Z_G(Q, Q_s; \mathbf{v}) = Q^{|V|/2} \sum_{A \subseteq E} Q^{\ell(A)/2} \left( \frac{Q_s}{Q} \right)^{\ell_s(A)} \prod_{e \in A} x_e \quad (3)$$

where we have introduced  $x_e = Q^{-1/2} v_e$ . In other words, the weight of a bulk loop (resp. a boundary loop) is  $n$  (resp.  $n_s$ ), subject to the relations

$$Q = n^2 \quad Q_s = n n_s \quad (4)$$

The boundary loop model (3) was introduced in [2], and further studied in a more general setting in [4]. The emphasis in Refs. [2, 4] was on the ferromagnetic case where all  $x_e = 1$ . We shall see now that the generalization of these results to the antiferromagnetic region (with  $x_e < 0$ ) allows to infer the phase diagram of the boundary chromatic polynomial.

### 3 Beraha-Kahane-Weiss theorem

We wish to study the boundary chromatic polynomial in the thermodynamic limit where  $G$  becomes large ( $|V| \rightarrow \infty$ ). In general, one may take the limit  $|V| \rightarrow \infty$  through a recursive family of graphs  $G_N$  embedded in the annulus, of width  $W$  and circumference  $N$ , such that  $|V| \sim NW$  and  $|V_s| \sim N$ . In particular one may think of strips of regular lattices (square, triangular, ...), but we emphasize that most of our results do not depend on the detailed structure of the graph, nor do they require that it be regular.

In section 4 we take the width  $W \propto N$ , so that the limiting graph  $G_\infty$  is two-dimensional, and the results [2] of conformal field theory (CFT) apply. In section 5, we consider instead  $W$  finite, so that  $G_\infty$  is quasi one-dimensional, and we shall see that the main results hold true in that case as well.

In both cases one may think of the partition function  $P_G(Q, Q_s)$  as being built up by a transfer matrix, with time slices containing  $W$  spins. The structure of the transfer matrix has been discussed in details in [2], and in particular it was shown that each of its eigenvalues  $\lambda_i$  contributes to the

partition function with a non-trivial multiplicity  $D_i$  that we shall refer to as an *eigenvalue amplitude*. Hence,

$$P_G(Q, Q_s) = \sum_i D_i(\lambda_i)^N. \quad (5)$$

The fact that  $D_i \neq 1$  in general can be traced back to the non-local nature of the loops defining (3), and to the periodic boundary conditions in the time direction.

We wish to study the phase diagram of the boundary chromatic polynomial by locating the accumulation points  $\mathcal{A}$  of the partition function zeroes  $P_G(Q, Q_s) = 0$  in the limit  $N \rightarrow \infty$ . Following Lee and Yang [5], this can be done by fixing one of the variables  $Q$  or  $Q_s$  (or by imposing a fixed relation among  $Q$  and  $Q_s$ ), and letting the remaining variable (henceforth denoted  $z$ ) take complex values.

Due to the form (5) the Beraha-Kahane-Weiss (BKW) theorem [6] applies. Let us call an eigenvalue  $\lambda_i$  dominant at  $z$  if  $|\lambda_i(z)| \geq |\lambda_k(z)|$  for all  $k$ . The BKW theorem then states that (under very mild assumptions)

- $z \in \mathcal{A}$  is an isolated accumulation point iff there is a *unique* dominant eigenvalue  $\lambda_i$  at  $z$  and the corresponding amplitude vanishes,  $\alpha_i(z) = 0$ .
- $z \in \mathcal{A}$  forms part of a continuous curve of accumulation points iff there are *at least two* dominant eigenvalues at  $z$ . (In other words,  $z$  is the locus of a level crossing involving a dominant eigenvalue.)

It is not in general clear to what extent CFT predictions apply to complex values of the parameters  $Q$  and  $Q_s$ . But at least we can infer important information about the phase diagram by combining the BKW theorem [6] with the CFT results [2] for the special case of real parameter values.

## 4 Phase diagram in the thermodynamic limit

It is useful to parametrize the bulk and boundary loop weights as follows

$$n = 2 \cos(\pi e_0), \quad n_s = \frac{\sin((r+1)\pi e_0)}{\sin(r\pi e_0)} \quad (6)$$

defining the parameters  $e_0$  and  $r \in (0, \frac{1}{e_0})$ . The continuum theory then has central charge

$$c = 1 - \frac{6e_0^2}{1 - e_0} \quad (7)$$

The range  $e_0 \in [0, \frac{1}{2})$  describes the usual ferromagnetic-paramagnetic transition, corresponding to positive values of  $n$  and  $n_s$ .

We here need the analytic continuation into the range  $e_0 \in (\frac{1}{2}, 1)$ , where  $n$  and  $n_s$  become negative. This range was referred to as the Berker-Kadanoff (BK) phase in [7]. Inspecting Fig. 2 it is easy to see that (3) is invariant under a simultaneous sign change of  $n$ ,  $n_s$ , and  $x_e$ . The BK phase therefore corresponds to negative values of  $x_e$ , i.e., it describes a part of the antiferromagnetic region of the Potts model. Its relevance to the chromatic line  $v_e = -1$  is due to the fact that the temperature variable  $v_e$  is an *irrelevant* perturbation in the BK phase, in the sense of the renormalization group. The BK phase therefore controls, for any fixed  $Q \in (0, 4)$ , a *finite* range of values  $v_e$ . One may therefore expect that at least for  $Q < Q_c$ , where  $Q_c \leq 4$  is some lattice-dependent constant, the BK phase will control the chromatic line  $v_e = -1$ .

To give a little more substance to this general discussion, it is worthwhile to recall some exact information about the special cases of the square and triangular lattices. The standard Potts model ( $Q_s = Q$  and  $v_e = v$ ) is then exactly solvable on the curves [8, 9]

$$\begin{aligned} v^2 &= Q && \text{(square lattice)} \\ v^3 + 3v^2 &= Q && \text{(triangular lattice)} \end{aligned} \tag{8}$$

In view of the parametrization (6) it is more convenient to rewrite this as

$$\begin{aligned} v &= 2 \cos(\pi e_0) && \text{(square lattice)} \\ v &= -1 + 2 \cos\left(\frac{2\pi e_0}{3}\right) && \text{(triangular lattice)} \end{aligned} \tag{9}$$

where  $e_0 \in [0, 1]$  for the square lattice and  $e_0 \in [0, \frac{3}{2}]$  for the triangular lattice.

Both analytical and numerical studies of the Potts model with  $Q_s = Q$  and either free or periodic transverse boundary conditions conclude that the critical exponents along the curves (8) for  $e_0 \in [0, 1)$  are those predicted by the CFT. In particular, the central charge is (7) as claimed. Moreover, the exponents for  $e_0 \in (\frac{1}{2}, 1)$  are just the analytic continuations of those valid for the usual ferromagnetic regime  $e_0 \in (0, \frac{1}{2})$ . This already strongly suggests that the critical properties for  $e_0 \in [0, 1)$  are lattice-independent (universal).<sup>1</sup> This conclusion is further corroborated by the so-called Coulomb gas approach [10] to CFT.

---

<sup>1</sup>In the case of the triangular lattice, the range  $e_0 \in (1, \frac{3}{2}]$  describes a very different CFT [11] which we shall not need further in the present work.

Further studies have established that for each  $Q \in (0, Q_c)$  the chromatic polynomial indeed renormalizes to the BK phase, with the following values of  $Q_c$  for the square [12] and triangular [13, 14] lattices

$$\begin{aligned} Q_c &= 3 && \text{(square lattice)} \\ Q_c &= 3.8196717312 \dots && \text{(triangular lattice)} \end{aligned} \tag{10}$$

We now return to the main objective of this section, which is to establish the critical behavior of the boundary chromatic polynomial. On general grounds, boundary conditions should not modify bulk RG flows.<sup>2</sup> Therefore, we expect the analytic continuation of the CFT results [2] to the range  $e_0 \in (\frac{1}{2}, 1)$  to describe the critical behavior of the boundary chromatic polynomial for  $Q \in (0, Q_c)$ .

It is convenient to set  $e_0 = 1 - \frac{1}{t}$ , so that the BK phase corresponds to  $t > 2$ . The parameter  $r$  appearing in (6) is then constrained to  $r \in (0, \frac{t}{t-1})$ . We have

$$\begin{aligned} n &= -2 \cos\left(\frac{\pi}{t}\right) \\ n_s &= -\frac{\sin\left(\frac{(r(t-1)-1)\pi}{t}\right)}{\sin\left(\frac{r(t-1)\pi}{t}\right)} \end{aligned} \tag{11}$$

In this parametrization,  $Q = n^2$  [see Eq. (4)] is nothing else than the  $t$ 'th Beraha number  $B_t$  defined in (2). Real chromatic zeroes have long been known [3] to accumulate around  $B_t$  for integer values of  $t \geq 2$ . One major motivation of this work is to show that the special role played by the Beraha numbers is destroyed by choosing  $Q_s \neq Q$ .

As explained in [2] the detailed transfer matrix structure implies that each eigenvalue appearing in (5) is in fact an eigenvalue of a modified transfer matrix in which the number of loops winding around the periodic direction of the annulus (i.e., which are non-homotopic to a point) is fixed. Each eigenvalue can thus be labelled by the corresponding number of winding loops

---

<sup>2</sup>This is of course a subtle issue in cases such as this one, where the statistical models are not very physical. In fact, there *are* some boundary terms that can profoundly affect the behavior of flows in the Berker-Kadanoff phase—for instance those breaking the quantum group symmetry in the XXZ chain version of the models. For the boundary terms we are considering however—which can be described through the boundary Temperley Lie algebra—no such “rogue” behavior seems to occur.



$L = 0, 2, 4, \dots$ , as  $\lambda_i^{(L)}$ . By the definition of the Potts model and the medial graph  $\mathcal{M}$ , the corresponding number of winding clusters is  $L/2$ . In each sector with  $L > 0$ , the dominant eigenvalue corresponds to the outermost of the winding loops being constrained to be a boundary loop (i.e., we can restrict to what was called the “blobbed sector” in [2, 4]).

The existence of  $L$  winding loops corresponds in CFT to the insertion of a pair of so-called  $L$ -leg operators  $\mathcal{O}_L$  at the extremities of the strip; the extremities are subsequently glued together to form the annulus with periodic boundary conditions in the time direction. The asymptotic scaling for  $W \gg 1$  of the dominant eigenvalue  $\lambda_0^{(L)}$  in each sector  $L$  is then fixed by CFT as [15]

$$\frac{\lambda_0^{(L)}}{\lambda_0^{(0)}} = \exp\left(-\frac{\pi h_L}{W}\right) + \dots \quad (12)$$

where the dots on the right-hand side represent terms that decay faster than  $\exp(-\text{const}/W)$ .

The constant  $h_L$  appearing in (12) is the so-called conformal weight of the  $L$ -leg operator (in the “blobbed sector”) whose value has been established in [2, 16]. After the analytic continuation implied by the parametrization (11), this reads

$$h_L = \frac{1}{4t} \left( L^2 - 2rL(t-1) + (r^2 - 1)(t-1)^2 \right) \quad (13)$$

The corresponding eigenvalue amplitude has been derived rigorously in [2]:

$$D_L = \begin{cases} 1 & \text{for } L = 0 \\ n_s U_{L-1}(n/2) - U_{L-2}(n/2) & \text{for } L > 0 \end{cases} \quad (14)$$

where  $U_j(x)$  is the  $j$ 'th order Chebyshev polynomial of the second kind.

Note that in the probabilistic regime ( $e_0 \in [0, \frac{1}{2}]$ ) the continuum limit is dominated by  $L = 0$ . This is no longer true in the BK phase, where for any  $t$  there is at least one of the exponents  $h_L$  taking negative values. The most negative exponent determines the most “probable” number of winding loops. This situation is clearly counter-intuitive from a probabilistic point of view, but it is made possible by the appearance of negative Boltzmann weights. Note also that the invariance of (3) under a simultaneous sign change of  $n$ ,  $n_s$ , and  $x_e$  is not sufficient to make all weights positive.

Using (12), dominant level crossings of transfer matrix eigenvalues correspond asymptotically (for  $W \gg 1$ ) to level crossings of the conformal weights  $h_L$ . We can thus read directly from (13) the necessary and sufficient criterion

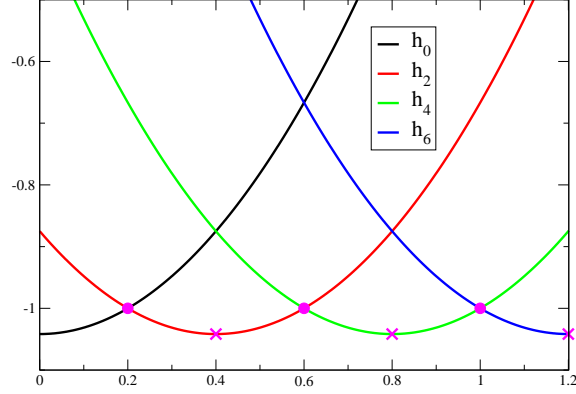


Figure 3: Conformal weights  $h_L$  as functions of the parameter  $r$  for the case  $t = 6$ . Dominant level crossings and vanishing dominant amplitudes are shown respectively as solid circles and crosses.

for the second part of the BKW theorem. Indeed, level crossings involving the dominant  $L$ -leg sector occur when

$$h_L = h_{L+2} \Leftrightarrow r = \frac{L+1}{t-1} \quad (15)$$

with  $L \leq t-1$ . In particular,  $h_L$  is the most negative exponent for  $r \in (\frac{L-1}{t-1}, \frac{L+1}{t-1})$ .

Similarly, the necessary and sufficient criterion for the first part of the BKW theorem is read off from (14). Indeed, the amplitude of the dominant  $L$ -leg sector vanishes when

$$D_L = 0 \Leftrightarrow r = \frac{L}{t-1} \quad (16)$$

with  $L = 2, 4, 6, \dots$

These phenomena are illustrated in Fig. 3 for the case  $t = 6$  (the  $Q = 3$  state Potts model).

For any fixed  $n$ , phase transitions will therefore take place for  $r = s/(t-1)$

and integer  $s \in (0, t]$ . The corresponding value of the boundary parameter is

$$n_s = -\frac{\sin\left(\frac{(s-1)\pi}{t}\right)}{\sin\left(\frac{s\pi}{t}\right)} \quad (17)$$

For even  $s$  this corresponds to a vanishing dominant amplitude, and for odd  $s$  to a dominant level crossing. The corresponding value of the dominant exponent (13) is  $h_L = -\frac{(t-1)^2}{4t}$  for any even  $s$ , and  $h_L = \frac{2-t}{4}$  for any odd  $s$ .

The  $N \rightarrow \infty$  limiting curve of accumulation points of partition function zeroes in the complex  $Q_s$  plane (in the vicinity of the real  $Q_s$  axis) can now be inferred from the BKW theorem: For even  $s$  one has an isolated real accumulation point, and for odd  $s$  a continuous curve of accumulation points intersects the real axis.

In the example  $t = 6$  of Fig. 3, the transitions at  $r = \frac{1}{5}, \frac{2}{5}, \frac{3}{5}, \frac{4}{5}, 1, \frac{6}{5}$  correspond to the following numbers of boundary colors:  $Q_s = 0, 1, \frac{3}{2}, 2, 3, \infty$ .

The discussion following (16) has subsumed that we are interested in the phase diagram for fixed  $Q$  and varying  $Q_s$ . But of course the criteria (15)–(16) for phase transitions hold true for other situations as well. In particular, the following few useful cases correspond to simple relations between  $r$  and  $t$ :

$$\begin{aligned} Q_s = Q & & : & r = 1 \\ Q_s = Q - 1 & & : & r = (t - 2)/(t - 1) \\ Q_s = Q - 2 & & : & r = (t - 2)/(2t - 2) \\ Q_s = Q - \sqrt{Q} & & : & r = 1/2 \\ Q_s = 0 & & : & r = 1/(t - 1) \\ Q_s = 1 & & : & r = 2/(t - 1) \\ Q_s = 2 & & : & r = (t + 2)/(2t - 2) \\ Q_s = \frac{1}{2}Q & & : & r = t/(2t - 2) \end{aligned} \quad (18)$$

For all of these, (15)–(16) yield phase transitions located at *integer* values of  $t$  (i.e., at the Beraha numbers  $B_t$ ), but this needs of course not be the case for more general choices of  $Q_s$ .

## 5 Quasi one-dimensional case

We now turn to the quasi one-dimensional geometry where the circumference of the annulus  $N \rightarrow \infty$ , while its width  $W$  is kept fixed and finite. In that case, the possible number of winding loops is constrained by  $L \leq 2W$ .

Eq. (14) for the eigenvalue amplitudes was in fact derived combinatorially for finite  $W$ , and so remains valid in this case. On the other hand, Eq. (13) must be discarded, since its derivation supposed the validity of conformal field theory. However, the pleasant surprise is that even for finite  $W$  the dominant eigenvalues in the  $L$  and  $(L + 2)$  leg sectors cross exactly for the values of  $r$  and  $t$  given by (15).

This coincidence follows from representation theory of the underlying boundary Temperley-Lieb algebra. While this algebra is semi-simple for generic values of the parameters, it admits families of degeneracy points where generically irreducible representations merge into larger indecomposable representations. Results in [17] guarantee that this occurs for finite values of  $W$  exactly at the same values that lead to the coincidences (15) of the conformal weights in the continuum limit.

When  $r = 1$ —in the original parametrization (6)—this can be understood somewhat more easily by using quantum group representation theory [18], as the generic  $U_q(sl(2))$  representations for sectors  $L$  and  $L + 2$ , of spin  $j = L/2$  and  $j = L/2 + 1$ , merge into larger indecomposable representations. When  $r$  is integer larger than one, this can be explained similarly by the construction of section 5 in Ref. [2]. Indeed, there the effect of the boundary weight  $n_s$  was obtained algebraically by adding  $r$  extra strands on the outside of the annulus, subject to the action of a certain symmetrizer. Thus, the boundary loop model (3) with  $r$  integer is a special case of the standard loop model in which only the weight  $n$  appears. The latter is known to have an  $U_q(sl(2))$  quantum group symmetry [18], and this in fact implies that (15) still holds true. The presence of exact coincidences at arbitrary  $r$  can maybe be interpreted in terms of some quantum group—the commutant of the boundary Temperley-Lieb algebra—but we will not discuss this here.

The key results of section 4 therefore remain valid, up to two subtle effects to be discussed below.

To make this conclusion more accessible to readers unacquainted with quantum groups we turn to a numerical verification. Fig. 4 shows the leading free energies  $f_L = -\frac{1}{W} \log \lambda_0^{(L)}$  in the  $L$ -leg sector, as functions of  $r$  in the parametrization (11), for four different values of  $W$ . The results were obtained for the square lattice in the diagonal geometry defined in [2], along the curve (9) with  $e_0 \in (\frac{1}{2}, 1)$ , i.e., within the BK phase. Results for other lattices would be similar, provided that one remains inside the domain of attraction of the BK phase.

For each  $W$ , the dominant level crossings are seen to occur exactly as

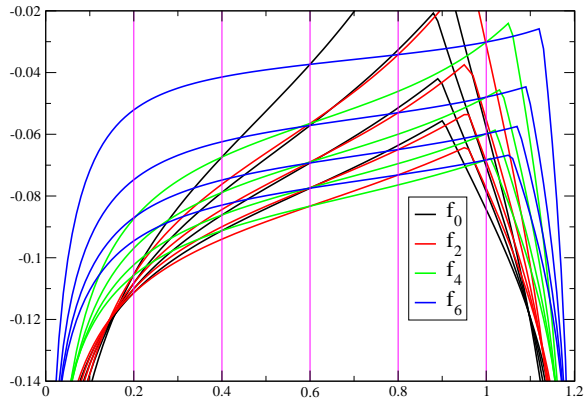


Figure 4: Leading free energies  $f_L$  in the sectors  $L = 0, 2, 4, 6$  as functions of  $r \in (0, \frac{6}{5})$ . The boundary loop model is here defined on the square lattice, along the BK critical curve, and the parameter  $t = 6$ . Four different system sizes ( $W = 8, 10, 12, 14$ ) are shown, the largest size corresponding to the lowermost curves. The vertical lines are guides to the eye.

predicted by (15). More generally, the  $r$  values singled out by (15)–(16) are seen to be the loci of subdominant level crossings as well, as would be expected from an underlying quantum group symmetry.

Fig. 4 was made for the choice  $t = 6$  (the  $Q = 3$  state Potts model), so that it is the precise finite-size analogue of Fig. 3. Other, non-integer choices of  $t$  were found to lead to the same conclusions.

We still need to discuss the two subtle effects referred to above. The first one is that if the annulus is too narrow ( $2W < \lfloor t \rfloor$ ) to accommodate the number of legs required by dominant sector with the largest  $L$  predicted by (15), the corresponding level crossings will simply be absent, and the  $2W$ -leg sector will remain dominant for the corresponding values of the parameter  $r$ .

The second effect is that Fig. 4 gives clear evidence that when  $r$  becomes too large, there is an internal level crossing in each  $L$ -leg sector, visible as a cusp in the curves. To the right of these cusps the pattern of dominance may change. A detailed analysis of the loci of the cusps reveals that their position tends to  $r = 1$  as  $W \rightarrow \infty$ , independently of the value of  $L$ . Moreover, for  $r \in (1, \frac{t}{t-1})$  it is the  $L = 0$  sector that will be dominant for large enough  $W$ .

## 6 Numerical verifications

To conclude this paper, we wish to check that the predictions of sections 4–5 agree with existing numerical results on the limiting curves  $\mathcal{A}$  of chromatic zeroes. The goal of this comparison is furthermore to convince the reader that our results are:

1. Lattice independent;
2. Independent of  $v_e$ , as long as we are in the BK phase;
3. Correct for various choices of  $Q_s$ .

Fig. 5 shows the accumulation points  $\mathcal{A}$  for the triangular-lattice chromatic polynomial on an annulus of width  $W = 7$ . Transverse boundary conditions are free, so that  $Q_s = Q$ . The agreement with the predictions (15)–(16) for the real accumulation points is perfect. There is one additional real accumulation point at  $Q_c(W) = 3.4682618071 \dots$  which is a finite-size analogue of  $Q_c$  discussed in section 4. As  $W \rightarrow \infty$  we expect  $Q_c(W) \rightarrow Q_c$  given by (10).

Zeros tri lattice  $L_x = 7_R$

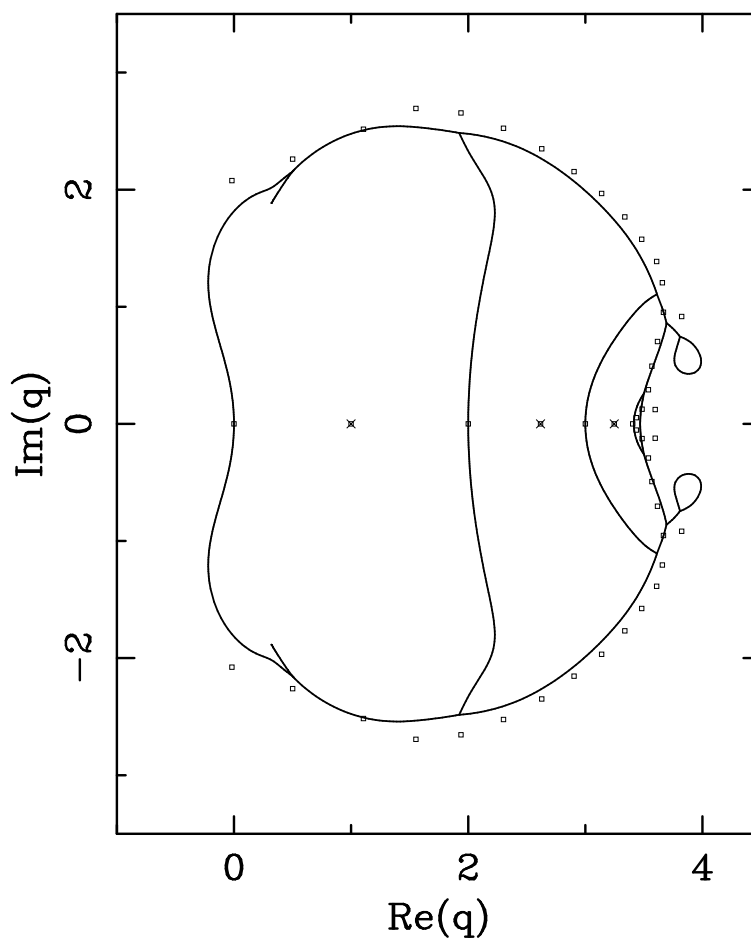


Figure 5: Zeroes in the complex  $Q$  plane of the triangular-lattice chromatic polynomial on an  $W \times N$  annulus for  $W = 7$  and  $N = 35$ , and their accumulation points as  $N \rightarrow \infty$ . The boundary parameter  $Q_s = Q$ . Taken from Figure 7 of Ref. [19].

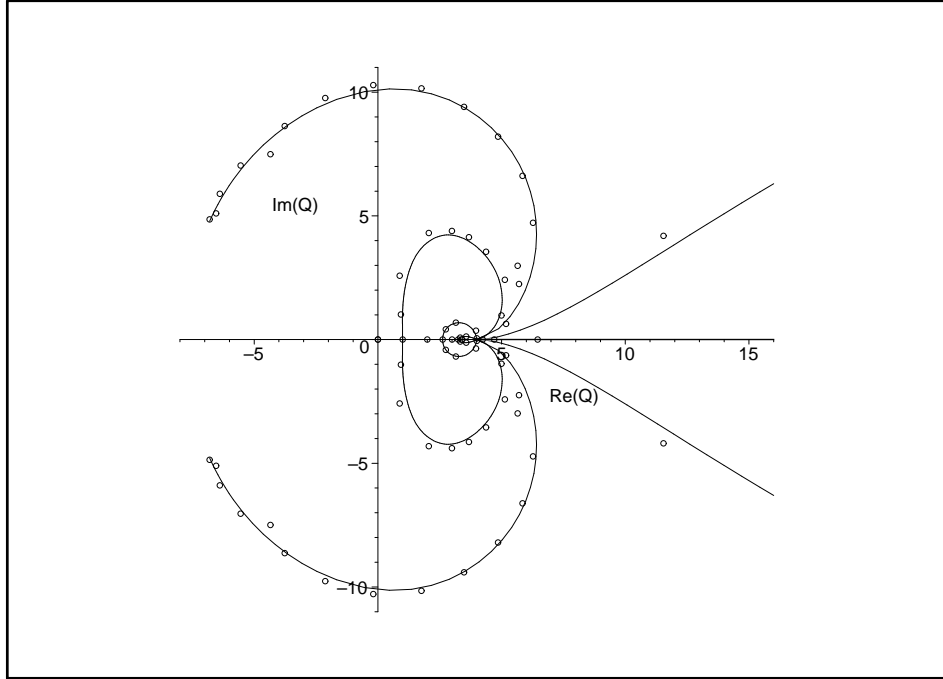


Figure 6: Zeroes in the complex  $Q$  plane of a square-lattice Potts model along the curve (8) on an  $W \times N$  annulus for  $W = 3$  and  $N = 26$ , and their accumulation points as  $N \rightarrow \infty$ . The boundary parameter  $Q_s = Q - 1$ . Taken from Figure 5 of Ref. [20].



Fig. 6 shows the accumulation points  $\mathcal{A}$  of partition function zeroes for a square-lattice Potts model along the curve (8). The geometry is that of an annulus of width  $W = 3$  with free transverse boundary conditions. However, all vertices on the outer rim of the annulus are connected to an extra exterior vertex. Therefore, the vertices on the outer rim (call them  $V_s$ ) support spins which are effectively constrained to take only  $Q_s = Q - 1$  different values (since they must be different from the value of the exterior spin). The partition function on the graph just described is therefore equal to  $QZ_G(Q, Q_s = Q - 1; v_e = \pm\sqrt{Q})$  in our notation, where now  $G$  is just an ordinary annulus of width  $W$ , with no extra exterior vertex.

Once again, the agreement with the predictions (15)–(16) for the real accumulation points is perfect. In particular, it follows easily from the predictions that the loci of isolated real accumulation points and curves of accumulation points intersecting the real  $Q$ -axis are swapped between Figs. 5 and 6. Along the curve (8) we would expect the BK phase to terminate only at  $Q_c = 4$ . Thus, the phase transition corresponding to the largest possible  $L$ -sector becoming dominant is limited by the available width as  $L \leq 2W$ . This is again in perfect agreement with Fig. 6. Similar agreements are found with the numerical results for real accumulation points given in [20] in the case  $W = 4$  (for which the complete limiting curve  $\mathcal{A}$  was not computed).

As a final check, we have computed the boundary chromatic polynomials with  $Q_s = Q - 2$  on an  $W \times N$  annulus for  $W = 2$  and  $N = 100$ , for both the square and the triangular lattice. Their zeroes in the complex  $Q$  plane are shown in Fig. 7. The agreement between Eqs. (15)–(16) and the real accumulation points for the triangular lattice is striking. Notice in particular that we predict in general that only Beraha numbers of even order, viz.  $B_t$  with  $t = 4, 6, 8, 10, \dots$ , can appear as accumulation points on the real  $Q$  axis. For the square lattice, the branch cutting the real axis at  $Q = 3$  marks the termination of the BK phase, in agreement with (10); to the right of this branch one does not observe any further structure as expected.

## 7 Conclusion

To summarize, we have introduced a new graph coloring problem—the boundary chromatic polynomial—and identified the loci of phase transitions for real values of the parameters  $Q$  and  $Q_s$ . Our results are lattice independent, and valid not only on the chromatic line but in the entire Berker-Kadanoff phase.

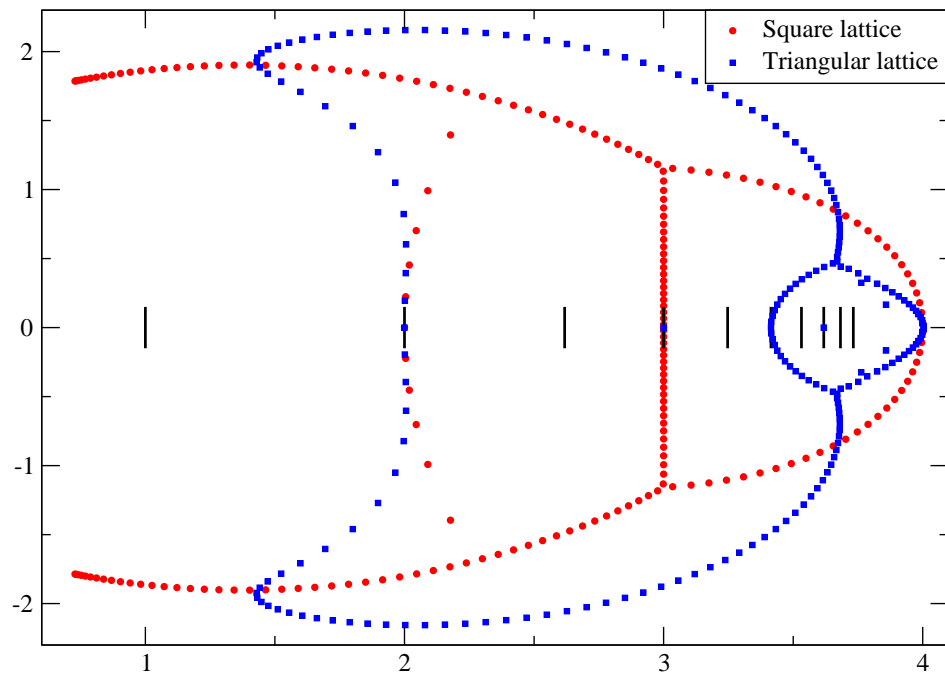


Figure 7: Zeroes in the complex  $Q$  plane of the  $Q_s = Q - 2$  boundary chromatic polynomials on an  $W \times N$  annulus, with  $W = 2$  and  $N = 100$ , for both the square and the triangular lattice. The black vertical lines indicate the positions of the Beraha numbers (2).

While we have provided a number of striking numerical tests that validate our analytical predictions, we believe we have left ample space for further numerical investigations of the boundary chromatic zeroes for families of graphs embedded in the annulus.

A straightforward extension of the work presented here would be to consider graphs on an annulus for which bulk spins can take values  $1, 2, \dots, Q$ , whereas spins on the outer (resp. inner) rim of the annulus are constrained to take values  $1, 2, \dots, Q_o$  (resp.  $1, 2, \dots, Q_i$ ). Note that in the cluster expansion analogous to (1), the number of spin values accessible to clusters touching both rims can be taken as a further independent variable  $Q_b$ , not necessarily equal to  $\min(Q_o, Q_i)$ .

Recent work on the corresponding two-boundary loop model furnishes the results for the eigenvalue amplitudes [4] and the critical exponents [21], analogous to (13)–(14) of this article. The phase diagram for real parameter values  $Q, Q_o, Q_i, Q_b$  can therefore be worked out along the lines presented here.

## Acknowledgments

We thank the authors of Refs. [19, 20] for the permission to reproduce Figs. 5–6. This work was supported by the European Community Network ENRAGE (grant MRTN-CT-2004-005616), by the Agence Nationale de la Recherche (grant ANR-06-BLAN-0124-03), and by the European Science Foundation network program INSTANS. One of us (JLJ) further thanks the Isaac Newton Institute for Mathematical Sciences, where part of this work was done, for hospitality.

## References

- [1] P.W. Kasteleyn and C.M. Fortuin, *J. Phys. Soc. Japan* **26** (Suppl.), 11 (1969); C.M. Fortuin and P.W. Kasteleyn, *Physica* **57**, 536 (1972).
- [2] J.L. Jacobsen and H. Saleur, *Nucl. Phys. B* **788**, 137–166 (2008); math-ph/0611078.
- [3] For an exhaustive list of references (as of December 2000), see: J. Salas and A. Sokal, *J. Stat. Phys.* **104**, 609–699 (2001); cond-mat/0004330.

- [4] J.L. Jacobsen and H. Saleur, J. Stat. Mech. P01021 (2008); arXiv:0709.0812.
- [5] C.N. Yang and T.D. Lee, Phys. Rev. **87**, 404 (1952).
- [6] S. Beraha, J. Kahane and N.J. Weiss, Proc. Nat. Acad. Sci USA **72**, 4209 (1975).
- [7] H. Saleur, Commun. Math. Phys. **132**, 657 (1990); Nucl. Phys. B **360**, 219 (1991).
- [8] R.J. Baxter, J. Phys. C **6**, L445–L448.
- [9] R.J. Baxter, H.N.V. Temperley, and S.E. Ashley, Proc. Roy. Soc. London A **358**, 535–559 (1978).
- [10] B. Nienhuis, in *Phase transitions and critical phenomena*, edited by C. Domb and J.L. Lebowitz (Academic, London, 1987), Vol. 11.
- [11] J.L. Jacobsen and H. Saleur, Nucl. Phys. B **743**, 207–248 (2006); cond-mat/0512058.
- [12] R.J. Baxter, Proc. Roy. Soc. London A **383**, 43–54 (1982).
- [13] R.J. Baxter, J. Phys. A **19**, 2821 (1986); *ibid.* **20**, 5241 (1987).
- [14] J.L. Jacobsen and J. Salas, Nucl. Phys. B **783**, 238–296 (2007); cond-mat/0703228.
- [15] J.L. Cardy, J. Phys. A **17**, L385 (1984).
- [16] I. Kostov, J. Stat. Mech. P08023 (2007); hep-th/0703221.
- [17] P. Martin and H. Saleur, Lett. Math. Phys. **30** 189 (1994).
- [18] V. Pasquier and H. Saleur, Nucl. Phys. B **330**, 523–556 (1990).
- [19] J.L. Jacobsen and J. Salas, J. Stat. Phys. **122**, 705–760 (2006); cond-mat/0407444.
- [20] S.-C. Chang and R. Shrock, Int. J. Mod. Phys. B **21**, 1755–1773 (2007); cond-mat/0602178.
- [21] J. Dubail, J.L. Jacobsen and H. Saleur (to be published).